Ruiz-Carrillo, A., Puigdomênech, P., Eder, G., & Lurz, R. (1980) *Biochemistry 19*, 2544–2554.
Schwert, G. W., & Takenaka, Y. (1955) *Biochim. Biophys. Acta 16*, 570–583.
Shick, V. V., Belyavsky, A. V., Bavykin, S. G., & Mirzabekov, A. D. (1980) *J. Mol. Biol. 139*, 491–517.
Simpson, R. T., & Whitlock, J. P., (1976) *Cell (Cambridge, Mass.) 9*, 347–353.
Stein, A., Whitlock, J. P., & Bina, M. (1979) *Proc. Natl. Acad. Sci. U.S.A. 76*, 5000–5004.
Tatchell, K., & van Holde, K. E. (1979) *Biochemistry 18*, 2871–2880.
Thomas, J. O. (1984) *J. Cell. Sci. Suppl. 1*, 1–20.
Weintraub, H., & van Lente, F. (1974) *Proc. Natl. Acad. Sci. U.S.A. 71*, 4249–4253.
Whitlock, J. P., & Simpson, R. T. (1977) *J. Biol. Chem. 252*, 6516–6520.
Whitlock, J. P., & Stein, A. (1978) *J. Biol. Chem. 253*, 3857–3861.
Wilhelm, M. L., & Wilhelm, F. X. (1980) *Biochemistry 19*, 4327–4331.
Yager, T. D., & van Holde, K. E. (1984) *J. Biol. Chem. 259*, 4212–4222.
Zama, M., Bryan, P. N., Harrington, R. E., Olins, A. L., & Olins, D. E. (1978a) *Cold Spring Harbor Symp. Quant. Biol. 42*, 31–41.
Zama, M., Olins, D. E., Prescott, B., & Thomas, G. J. (1978b) *Nucleic Acids Res. 5*, 3881–3897.
Zayetz, V. W., Bavykin, S. G., Karpov, V. L., & Mirzabekov, A. D. (1981) *Nucleic Acids Res. 9*, 1053–1068.

# Effects of Hydration on Purine Motion in Solid DNA†

Rolf Brandes, Regitze R. Vold, Robert L. Vold, and David R. Kearns*
*Department of Chemistry, University of California at San Diego, La Jolla, California 92093*
*Received June 12, 1986*

ABSTRACT: Deuterium quadrupole echo spectra and spin–lattice relaxation rates measured at 76.8 and 38.4 MHz as a function of relative humidity are reported for calf thymus DNA deuterated at positions A8 and G8. The amplitude of base pair motion is observed to increase slightly with increasing degree of hydration (up to ~20 mol of $H_2O$/nucleotide), and the onset of motion is associated with a more than 100-fold drop in $T_1$. This observed decrease in $T_1$ parallels that observed previously for the phosphate backbone and appears to be characteristic of collective modes of motion. Above ~20 mol of $H_2O$/nucleotide, the amplitude of the base motion increases substantially up to a point where slow components of motion lead to a complete loss of the quadrupole echo.

The conformational flexibility of polynucleotides in solution has been the subject of numerous studies (Cohen & Eisenberg, 1969; Allison & Schurr, 1979; Barkley & Zimm, 1979; Englander et al., 1980; Hogan & Jardetzky, 1980; Early et al., 1981; Keepers & James, 1982; Levy et al., 1983; Thomas & Schurr, 1983; Kearns, 1984) using several kinds of physicochemical techniques over the last few years, but significant questions about the nature of this internal mobility still remain to be answered. In particular, it remains to be established whether internal motions detected by NMR are "localized" (Bolton & James, 1980; Hogan & Jardetzky, 1980; Assa-Munt et al., 1984) or the result of longer range cooperative torsional and bending modes of the double helix (Allison & Schurr, 1979; Barkley & Zimm, 1979). The extent to which these motions are influenced by metal ions, hydration, or helix-binding agents is also not understood in detail. One difficulty associated with the interpretation of many measurements on DNA solutions is the presence of overall tumbling of the molecule, and accordingly, interest has developed in investigating solid DNA where the nature of internal motions may be more easily explored. Crystallographic measurements (Drew et al., 1980, 1982) have clearly shown that large thermal parameters are associated with atomic coordinates in fibrous and crystalline DNA. Recently, Holbrook and Kim (1984) used a "segmented rigid body" model to determine directions and magnitudes of translational and rotational motion of individual polynucleotide subgroups from single-crystal X-ray diffraction data. They find librational motions of the bases and ribose units with amplitudes up to ±20° and larger motions of the phosphate unit in solid samples of double- and single-stranded polynucleotides.

Solid-state NMR spectra and relaxation rates may be used to evaluate not just the amplitudes, but also the rates of internal motions in nucleic acids. During the last few years, several NMR studies of solid polynucleotides have been published. At present, it appears that $^{31}P$ (Shindo et al., 1980, 1983; DiVerdi & Opella, 1981; Nall et al., 1981; Opella et al., 1981; Mai et al., 1983; Fujiwara & Shindo, 1985) and $^{2}H$ (DiVerdi & Opella, 1981; Bendel et al., 1983; James et al., 1983; Vold et al., 1986) are the most readily accessible and informative nuclear spin probes. On the basis of the NMR reports available up to now, it appears that internal motion is quite limited in amplitude in dehydrated A-form DNA (Shindo et al., 1980; DiVerdi & Opella, 1981; Nall et al., 1981; Opella et al., 1981) but that the amplitudes of motion increase with increasing degree of hydration. Early studies (Shindo et al., 1980, 1983; DiVerdi & Opella, 1981; Nall et al., 1981; Opella et al., 1981) have shown that the phosphate backbone of hydrated B-form DNA undergoes rather large angular

† This research was supported by grants from the U.S. Public Health Service to R.R.V. and D.R.K. (Grant GM35177) and the National Science Foundation to R.L.V. and R.R.V. (Grant CHE84-21291). R.B. received a travel grant from the Department of Biophysics, University of Stockholm. We also acknowledge the aid of the California Institute of Technology Regional NMR Facility funded by the National Science Foundation (Grant CHE84-40137).

0006-2960/86/0425-7744$01.50/0 

excursions. So far, the most quantitative NMR study of internal motion in solid DNA was reported by Mai et al. (1983), who measured $^{31}P$ NMR spectra, spin–lattice relaxation rates, and NOE's in calf thymus DNA as a function of degree of hydration, from the dry A-form DNA to B-form DNA with 33 mol of water/nucleotide. The authors identify three distinct motional regimes, from high-frequency, low-amplitude motion at low water content through a slower, larger amplitude motion near the transition to B form to a final regime where complete averaging of the phosphorus shielding tensor occurs by virtue of very large amplitude motion. The conclusions by Mai et al. (1983) are in substantial agreement with the earlier, less complete observations as well as with a later report on heavily hydrated oriented DNA fibers by Fujiwara and Shindo (1985), who conclude that the very large amplitude motion at high humidity in fact results in reorientation of the DNA molecule about its long axis.

Whether the motion observed at different levels of humidity is local or collective in nature remains open to question. Most nuclear spin relaxation experiments provide information only about the reorientational motion of *individual* spin interaction tensors, and the question can therefore be settled only indirectly by NMR techniques, via the interpretation of extensive measurements of the frequency and temperature dependence of relaxation rates in terms of collective vs. independent segmental models of motion. While sufficient data for this purpose are not yet available, a comparison of relaxation data obtained as a function of frequency for different subunits of the polynucleotide should throw some light on the issue. Early observations on DNA deuterated in the purine 8-positions (Opella et al., 1981) suggested that the base pairs remain immobile under conditions where the phosphodiester groups undergo significant motion. However, James and co-workers (Bendel et al., 1983; James et al., 1983) found, using deuterium NMR spectroscopy, that limited amplitude motion takes place in hydrated fibers of poly(I)·poly(C) deuterated in the inosine 8-position, and the presence of low amplitude librational base pair motion was recently demonstrated (Vold et al., 1986) in partially hydrated, oriented samples of A- and B-form DNA.

In order to determine to which extent the motion of the base pairs is correlated with the motion of the phosphate backbone, we have measured the deuterium NMR line shapes and spin–lattice relaxation rates for double-stranded, high molecular weight calf thymus DNA at various levels of hydration up to 22 mol of $H_2O$/nucleotide. Our results confirm that the DNA bases execute restricted, but significant librational motion. We find that this motion strongly affects the deuterium spin–lattice relaxation rates and that this motion echoes the increase in mobility observed for the phosphate groups (Mai et al., 1983).

## Materials and Methods

High molecular weight calf thymus DNA (Sigma D-1501) was dissolved in a $D_2O$ buffer [1 M NaCl, 0.04 M cacodylic acid, 0.01 M ethylenediaminetetraacetic acid (EDTA), pD 7.3] to a concentration of ~20 mg/mL (resulting in a gelatinous solution). Protons on the 8-position of guanine and adenine were exchanged with deuterons by incubating the sample at 68 °C for 10 days (Brandes & Ehrenberg, 1986). To control the salt concentration, precipitated, deuteron-exchanged DNA was equilibrated in an ethanol–water mixture containing either 75% EtOH–0.03 M NaCl or 80% EtOH–0.25 M LiCl to obtain DNA with either Na or Li as the counterion. This produces an excess salt concentration of 1.2% by weight for the Na-DNA and 5.9% for the Li-DNA (Rupprecht & Forslind, 1970). Two different drying procedures were used for each DNA type: lyophilization of the DNA solution or slow evaporation of the water for ~1 day in an oven held at 45 °C, material henceforth referred to as oven-dried DNA. Lyophilization produced a white, fluffy, cotton-like preparation, which was difficult to pack into a 5-mm NMR tube. Twice as much oven-dried DNA (ca. 80 mg) could be packed into an NMR tube and contained within the radio-frequency coil since this material was more compact than the lyophilized DNA.

To determine the dry weight of the samples, they were first equilibrated for 3 weeks at a fixed relative humidity (RH) over salt solutions of known vapor pressure (Weast, 1971), namely, 66% RH for the Li-DNA samples and 75% RH for the Na-DNA samples. The water adsorption at these humidities has been carefully determined (Rupprecht & Forslind, 1970) and may be expressed as

$$m(\mathrm{RH}) = m_{\mathrm{dry}}[1 + f(\mathrm{RH})] \quad (1)$$

where $m_{\mathrm{dry}}$ is the dry weight, $m(\mathrm{RH})$ is the weight of DNA equilibrated at 66% or 75% RH, and $f(\mathrm{RH})$ is the fractional water adsorption that depends on the relative humidity (and salt content). For the samples used here $f(66\%) = 0.42$ and $f(75\%) = 0.46$. The procedure described above was used to avoid problems of removing all water from the DNA, since this sometimes has proved to be difficult. Thus, a sample that was subjected to vacuum pumping for 12 h still contained some residual water that could only be removed by extensive pumping at 100 °C (Rupprecht & Forslind, 1970).

The NMR samples were then hydrated over appropriate saturated salt solutions (Weast, 1971) to produce the relative humidities given in Table I. Hysteresis effects on adsorption/desorption (Falk et al., 1962) were avoided by drying the samples over $P_2O_5$ for 10 days before rehydrating them at their appropriate relative humidities. After 4 weeks of equilibration, the rehydrated weight was used to calculate the water adsorption for each sample (Figure 1).

Deuterium NMR spectra were recorded at 38.4 and 76.8 MHz with quadrature-phase detection at 25 °C on two broad-band spectrometers, both interfaced to Nicolet 2090 oscilloscopes and 1280 computer systems. About 64 000 scans at 38.4 MHz and 4000 scans at 76.8 MHz with a Gaussian line broadening of 1–2 kHz were used to obtain adequate signal-to-noise ratio. Phase-cycled $\pi/2_x$–$\tau_1$–$\pi/2_y$–$\tau_2$–acq quadrupole echo sequences (Davis et al., 1976) were used with 2.0-$\mu$s (38.4 MHz) or 4.4-$\mu$s (76.8 MHz) $\pi/2$ pulses. The pulse spacing $\tau_1$ was usually 20–50 $\mu$s, and $\tau_2$ was adjusted separately to ensure sampling at the top of the echo. Spin–lattice relaxation times $T_1$ longer than 80 ms were determined by varying the repetition time between quadrupole echo sequences, while the inversion recovery technique was employed for shorter $T_1$ values. Transverse quadrupole echo decay times $T_{2E}$ were determined by varying the interpulse spacing of the quadrupole echo pulse sequence. For both $T_1$ and $T_{2E}$ we refer to time constants obtained by fitting the decays of the perpendicular edges (the "horns") of the powder patterns to appropriate, three-parameter exponential functions.

The temperature was measured in both spectrometers with thermocouples located near but outside the samples. At 38.4 MHz, the temperature can be assumed to be accurate within ±0.5 °C and 76.8 MHz to within ±1 °C. To exclude any possibility of a systematic temperature difference between the two spectrometers affecting the validity of the relaxation data, the sensitivity of $T_1$ to a 5 °C temperature increase was determined for Li-DNA at 75% RH and 76.8 MHz. As shown in Table I, the difference in $T_1$ at 25 and 30 °C was found to be (barely) within experimental error, and a possible 1–2

Table I: Deuterium Quadrupole Splittings and Relaxation Rates of Randomly Aligned DNA with $Na^+$ or $Li^+$ as Counterion[a]

| sample | % RH | $W$ (mol of $H_2O$/nucleotide) | 38.4 MHz | | 76.8 MHz | | $T_1$(76.8MHz)/$T_1$(38.4MHz) |
|---|---|---|---|---|---|---|---|
| | | | $\delta$ (kHz) | $T_1$ (s) | $T_1$ (s) | $T_{2e}$ ($\mu$s) | |
| Li-DNA | 0 | 1.4 | 126 ± 2 | | 7.3 ± 1.4 | | |
| | 6 | 2.8 | | | 4.2 ± 0.5 | | |
| | 35 | 4.5 | 123 ± 2 | 0.87 ± 0.04 | 2.0 ± 0.2 | | 2.3 ± 0.3 |
| | 52 | 6.3 | | | 0.62 ± 0.08 | 256 ± 25 | |
| | 66 | 7.7 | 122 ± 2 | 0.20 ± 0.01 | 0.38 ± 0.02 | 245 ± 42 | 1.9 ± 0.2 |
| | 75 | 9.8 | 122 ± 2 | 0.15 ± 0.01 | 0.26 ± 0.01 | 271 ± 24 | 1.7 ± 0.2 |
| | 75 | 9.8[b] | | | 0.22 ± 0.02 | | |
| | 75 | 10.0[c] | | | 0.26 ± 0.03 | | |
| | 84 | 12.1 | 119 ± 2 | 0.09 ± 0.02 | 0.20 ± 0.01 | 193 ± 17 | 2.2 ± 0.5 |
| | 88 | 19.7 | | | 0.068 ± 0.01 | 124 ± 33 | |
| | 92 | 22.6 | | | 0.062 ± 0.01 | 132 ± 16 | |
| Na-DNA | 66 | 7.2 | | | 0.30 ± 0.02 | | |
| | 75 | 8.4 | | | 0.27 ± 0.03 | | |
| | 84 | 9.8 | | | 0.21 ± 0.04 | | |
| | 92 | 20.8 | | | 0.045 ± 0.006 | | |

[a] Measurements were performed at 25 °C and various levels of hydration. [b] Measured at 30 °C. [c] Lyophilized DNA.

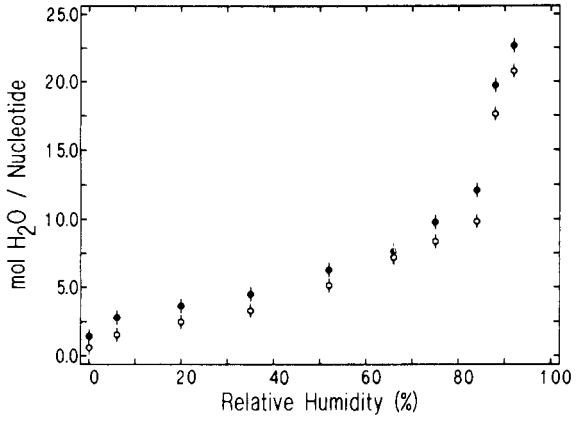


FIGURE 1: Variation of water content, $w$, of Na- (○) and Li-DNA (●) with relative humidity. The DNA samples were equilibrated at room temperature against saturated salt solutions producing a known constant relative humidity.

°C temperature difference between the two spectrometers is therefore insignificant.

The deuterium line-shape calculations (used in the simulations described below) were performed on a Celerity C1200 minicomputer. Fast librational averaging of $e^2qQ/h$ and $\eta$ described by Vold et al. (1986) was included in the line-shape calculations, and artifacts due to finite pulse widths were taken into account by using intensity corrections given by Bloom et al. (1980). A more detailed description of such calculations will be presented separately.

## Results

The relation between relative humidity and water content $w$ (in units of moles of $H_2O$ per nucleotide) is illustrated in Figure 1 for samples of oven-dried Na-DNA and Li-DNA. As can be seen, the Li-DNA samples adsorb more water at a given relative humidity than the Na-DNA samples, in part because of the higher salt content of the former. The water adsorption by the Na-DNA is similar to that reported earlier by Falk et al. (1962), and within experimental error no differences were observed between the water adsorption of lyophilized and that of oven-dried DNA at the same relative humidity.

For the Li-DNA sample hydrated at 75% RH, no difference in $T_1$ at 76.8 MHz was observed for samples prepared by lyophilization or oven-drying. Consequently, since better signal-to-noise was obtained from samples of oven-dried than of lyophilized DNA (because more oven-dried DNA could be packed in the NMR tube), subsequent measurements were performed on this material. The results are summarized in Table I.

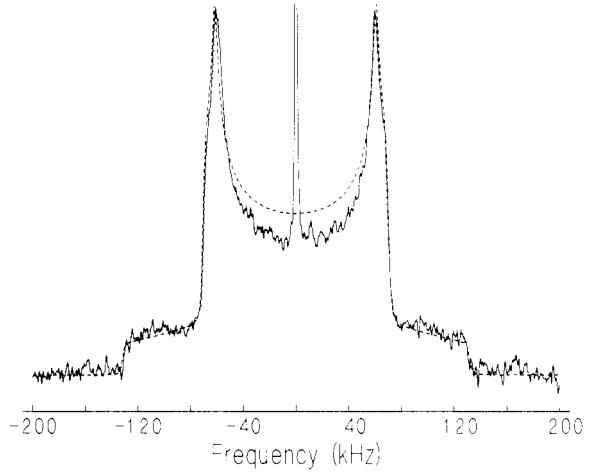


FIGURE 2: The 38.4-MHz deuterium quadrupole echo spectrum of Li-DNA at 66% RH ($w$ = 7.7) and 25 °C. The spectrum was obtained with 64 000 scans by using 2-$\mu$s $\pi/2$ pulses, and a 2-kHz Gaussian line broadening was applied to the free induction decay. The theoretical powder patterns were calculated from eq 4–6 of the text with libration angles $\theta_0,\phi_0$ = 6°,10° (dashed line) and $\theta_0,\phi_0$ = 10°,14°. The central narrow line is due to deuterium in the water of hydration.

An example of the deuterium NMR spectra of Li-DNA is presented in Figure 2. The spectrum was obtained at 38.4 MHz from a sample equilibrated at 66% RH ($w$ = 7.7), and the central spike, actually a narrow doublet, is due to deuterium present in the adsorbed (normal) water. The splitting between the perpendicular edges, the horns, of a powder pattern is given by

$$\delta = (3/4)(1 - \eta_{eff})(e^2qQ/h)_{eff} \quad (1a)$$

and is equal to 122 ± 2 kHz at this hydration level. The separation between the parallel edges (the "shoulders") is given by

$$\Delta = (3/2)(e^2qQ/h)_{eff} \quad (1b)$$

In principle, measurements of $\delta$ and $\Delta$ can be used to determine the effective quadrupole coupling parameters $(e^2qQ/h)_{eff}$ and $\eta_{eff}$. However, in practice, greater accuracy is achieved by simulation of the complete powder pattern. For the spectrum shown in Figure 2, simulation yields an observed quadrupole coupling constant $(e^2qQ/h)_{eff}$ = 173 ± 1 kHz and an asymmetry parameter $\eta_{eff}$ = 0.065 ± 0.010. Comparable values

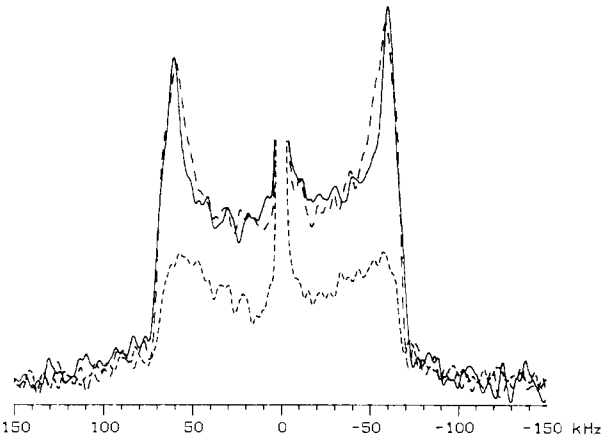


FIGURE 3: Deuterium quadrupole echo spectra of Li-DNA equilibrated at 75% (—), 84% (– –), and 88% (- - -) relative humidity recorded at 76.8 MHz and 25 °C with 4-$\mu$s $\pi/2$ pulses.

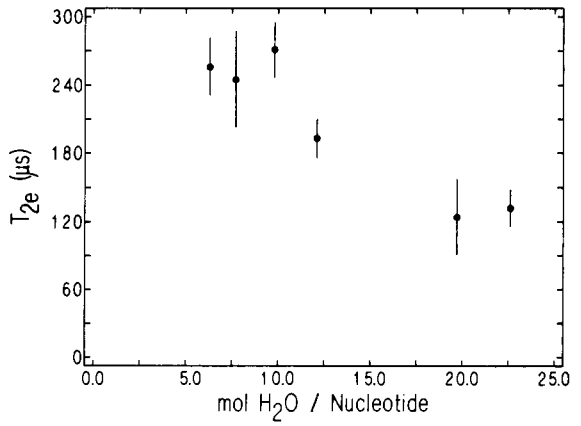


FIGURE 4: Effect of water content on the deuteron quadrupole echo decay time, $T_{2E}$, of Li-DNA.

for dry ($w \sim 1.4$) oriented Li-DNA are $(e^2qQ/h)_{eff} = 179 \pm 1$ kHz and $\eta_{eff} = 0.06 \pm 0.01$, corresponding to $\delta = 126 \pm 2$ kHz. At 84% RH ($w = 12$), this splitting has dropped to 119 kHz, which shows that the uptake of water is accompanied by increased amplitudes of motion of the bases.

Aside from the small reduction in the quadrupolar splitting (see Table I), no significant changes in the powder line shape were observed below 84% RH, but above this level the width of the horns (measured at 75% of maximum peak height) began to increase. As can be seen in Figure 3, the line-shape changes were accompanied by a serious loss in signal intensity, which ultimately, above 92% RH, led to complete loss of signal. A similar loss of the deuterium quadrupole echo was reported earlier by Bendel et al. (1983) for poly(I)·poly(C). The drop in quadrupole echo decay time $T_{2E}$ for Li-DNA as a function of $w$ is presented in Figure 4. At low levels of hydration, $T_{2E}$ may be partially determined by irreversible dephasing from coupling to surrounding protons, which are strongly coupled among themselves.

The most complete set of deuteron spin–lattice relaxation data vs. water content were obtained for the Li-DNA samples at 25 °C, and the results are summarized in Figure 5. It is known, on the basis of fiber diffraction patterns, that Li-DNA remains in the B-type conformation throughout the hydration range, at least down to 23% RH (Rupprecht & Forslind, 1970; Lindsey, 1986), and deuterium NMR spectra (unpublished results) on oriented fibers have demonstrated that the B-type conformation is retained to ~0% RH. At 76.8 MHz, a relaxation time $T_1 \sim 7$ s was obtained for the driest sample, for which $w = 1.4$. As the DNA becomes more hydrated, relaxation becomes more efficient, and between $w = 5$ and $w = 6$, $T_1$ drops particularly steeply. Further increase of the water content results in a monotonic decrease of the relaxation time, until $T_1 \sim 62$ ms at $w = 22$. Additional spin–lattice relaxation times were measured at 38.4 MHz in the range $w = 4.5$–12, and as indicated in Table I, the ratio $T_1(76.8)/T_1(38.4)$ was found to be approximately 2 for four different samples.

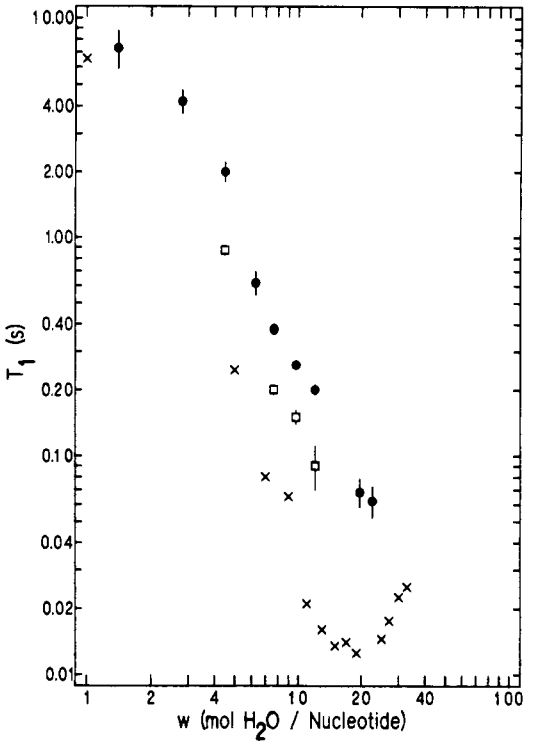


FIGURE 5: Deuterium spin–lattice relaxation times, $T_1$, as a function of hydration level, $w$, in moles of $H_2O$ per nucleotide. The solid circles (●) were measured at 76.8 MHz and the open squares (□) at 38.4 MHz for Li-DNA. The crosses (×) represent $^{31}P$ $T_1$'s obtained from Table I of Mai et al. (1983), divided by 20 for ease of comparison. Since the driest of those samples still contained some water, it has been assumed to contain 1 mol of $H_2O$/nucleotide.

For the Na-DNA samples, $T_1$ was only measured at 76.8 MHz for a few values of $w$. As shown in Table I, the Na-DNA samples, which are expected to undergo a transition from the A to the B form at 86–92% RH (Lindsey, 1986), appear to relax slightly faster (by at most 30%) than Li-DNA samples hydrated to the same water content. The quadrupolar splittings were, however, not discernibly different.

## Discussion

*Quadrupole Echo Spectra.* The decrease in quadrupolar splitting apparent from the data in Table I, $\delta = 126$ kHz at 0% RH and 119 kHz at 84% RH, shows that the amplitude of the librational motion of the base pairs increases as the DNA fibers are hydrated. The values quoted above for $(e^2qQ/h)_{eff}$ and $\eta_{eff}$ in dry Li-DNA are very similar to those obtained for a C-8 deuteron in purine nucleosides and nucleotide monophosphates (Tsang et al., 1986). The spin–lattice relaxation times are long, in the range 5–10 s, for both dry Li-DNA and the monomers. This implies that the density of motional fluctuations near the Larmor frequency is low in both of these types of materials, and we can consequently use either the dry DNA fiber or the nucleosides and nucleotides as reference materials for our analysis of the motion in the hydrated fibers.

The simplest way to account for the decrease in the effective quadrupole coupling constant is to assume that all librational

motion is fast compared to the width of the rigid lattice spectrum. The spectrum can then be simulated as a normal powder pattern with effective quadrupole coupling parameters calculated from an appropriate motional model. The simplest applicable model for the restricted motion of the CD bond is "diffusion-in-a-cone" (Warchol & Vaughan, 1978; Wang & Pecora, 1980; Lipari Szabo, 1981). The cone model makes no reference to any deviation from axial symmetry of either the molecular motion or the interaction tensor, but since the biaxiality is small in the present case, one might reasonably use the cone model to obtain an estimate of the extent of motion from the quadrupolar splittings. If we define $\theta_0$ as the half-angle of a cone with its axis ($z$) oriented along the time-averaged direction of the CD bond in a molecule-fixed frame, then the splitting between the powder pattern horns is given by

$$\delta = (3/4)(e^2qQ/h)_0 S_{zz} \quad (2)$$

where the (uniaxial) order parameter is given by

$$S_{zz} = (1/2)(\cos\theta_0)(1 + \cos\theta_0) \quad (3)$$

$(e^2qQ/h)_0$ refers to the quadrupole coupling constant in the absence of any polymer motion and is assumed equal to that measured for dry Li-DNA or the purine monomers. Application of this model to the observed decrease in quadrupolar splitting from 126 kHz at 0% RH to 122 kHz gives $S_{zz} = 0.968$ and $\theta_0 = 12°$ at 66% RH, while $S_{zz} = 0.944$ and $\theta_0 = 16°$ at 84% RH where the splitting has been reduced further to 119 kHz.

A more realistic approach recognizes the biaxial nature of the system, and the simplest model which takes this into account considers the base pairs as undergoing restricted diffusion in two perpendicular planes, one of which is the plane of the purine ring. As discussed previously (Vold et al., 1986), the frequency of a quadrupolar isochromat is then given by

$$\nu = \pm(3/4)(e^2qQ/h)_0[(1/2) \times (3\cos^2\beta - 1)f(\eta,\theta_0) - (1/2)(\sin^2\beta\cos 2\gamma)g(\eta,\theta_0,\phi_0)] \quad (4)$$

where

$$f(\eta,\theta_0) = (1/4)\left[1 - \eta - (3 + \eta)\frac{\sin 2\theta_0}{2\theta_0}\right] \quad (5)$$

and

$$g(\eta,\theta_0,\phi_0) = (1/4)\frac{\sin 2\phi_0}{2\phi_0}\left[3(\eta - 1) - (3 + \eta)\frac{\sin 2\theta_0}{2\theta_0}\right] \quad (6)$$

Here, $\beta$ is the angle between the DNA helix axis and the magnetic field, $\gamma$ is the angle of rotation of the CD vector around the DNA axis, and $\eta$ is the asymmetry parameter in the absence of motion. In this dual librational model, we have assumed that the CD bonds fluctuate uniformly over the intervals $(-\phi_0,+\phi_0)$ and $(90° - \theta_0,90° + \theta_0)$. The angles $\phi$ (in the purine plane) and $\theta$ (perpendicular to the purine plane) are defined such that eq 4–6 are consistent with the usual definition of $0 \leq \eta \leq 1$ for the nonaveraged quadrupole coupling tensor in aromatic molecules (Barnes, 1976).

In Figure 2 we have included two powder line shapes calculated from the frequency expression in eq 4–6 using $(e^2qQ/h)_0 = 179$ kHz and $\eta = 0.06$ with $\theta_0,\phi_0 = 6°,10°$ (dashed line) and $\theta_0,\phi_0 = 10°,14°$ (dotted line). The experimental spectrum falls somewhere between these two sets of values, which therefore serve as uncertainties in our estimate of the librational amplitudes, $\theta_0 = 8 \pm 2°$ and $\phi_0 = 12 \pm 2°$ at 66% RH. Note that this treatment gives amplitudes for the restricted motion that are not very different from that predicted from the cone model using only the observed splitting $\delta$.

If the librational motion responsible for the narrowing of the spectra is not fast, the approach described above is not appropriate. The line shape might then more properly be calculated with an exchange-type model in which the motion is simulated by jumps between a finite number of sites. Preliminary results indicate that spectra such as that shown in Figure 2 may in fact be more accurately simulated with either low-jump rates ($k \sim 10^3$–$10^4$ s$^{-1}$) or a distribution of rates among a limited number of sites with values of the polar angle, $\theta$, similar to those quoted above. Very low jump rates could not account for the decrease in $T_1$, but a distribution of rates is consistent with the frequency dependence of $T_1$ discussed below.

The 76.8 MHz spectra of Li-DNA equilibrated at the relative humidities of 75, 84 and 88% shown in Figure 3 illustrate the rapid loss of the quadrupole echo above 84% RH, even with pulse spacings as short as 20 $\mu$s. Crude but illustrative measurements of the quadrupole echo decay time $T_{2E}$ presented in Figure 4 provide a measure of this loss of signal, which above 92% RH renders the signal-to-noise unacceptably low. These results, when combined with earlier observations of complete narrowing of $^{31}$P spectra in Na-DNA above ~92% RH (Mai et al., 1983; Fujiwara & Shindo, 1985; Shindo et al., 1985), show that all parts of the DNA helix begin to undergo large amplitude motion at this level of hydration.

*Spin–Lattice Relaxation Times.* It is interesting to compare the effects of progressive hydration on the phosphate relaxation (in Na-DNA) with the purine deuteron relaxation (in Li-DNA). The results of the $^{31}$P relaxation measurements of Mai et al. (1983) have been included in Figure 5, where to facilitate the comparison the $^{31}$P $T_1$'s have been divided by 20. We will discuss four regions of hydration, $w$ = 0–6, 6–12, 12–20, and >20.

As DNA adsorbs water, the first five to six waters per nucleotide preferentially hydrate the phosphate oxygen atoms on the backbone (Falk et al., 1963). The decrease in relaxation time for both $^{31}$P and $^2$H is indicative of increased mobility, but the motion of bases as well as backbone is clearly highly restricted since neither the $^{31}$P nor $^2$H spectra show significant narrowing at these levels of hydration. For the bases, the analysis presented above shows that the maximum excursion below $w$ = 5–6 is ≤10°.

Between 6 and 12 mol of $H_2O$/nucleotide, hydration of the bases takes place (Falk et al., 1963), and it is worthwhile noting the apparent sharper drop in $T_1$ and change in slope that occurs near $w = 5$ (see Figure 5). In this range, Mai et al. (1983) concluded that the onset of a new motion was responsible for further reduction of $T_1$ since the $^{31}$P{$^1$H} NOE simultaneously decreased. This new motion was therefore believed to be slower, but still close to the Larmor frequency. Our deuterium data likewise suggest that the bases move into a new motional regime as they become hydrated. However, since the $T_1$ values at 38.4 MHz, in the range $w$ = 5–12, remain shorter than at 76.8 MHz by a nearly constant factor of 2 even though the $T_1$ values themselves change by a factor of ~10, the changes in these observations are not consistent with the onset of a "new slower motion" suggested by Mai et al. (1983).

Above $w = 12$, where the hydration of DNA is complete (Falk et al., 1962, 1963), a second layer of water molecules continues to indirectly hydrate the DNA by hydrogen bonding to the primary layer of bound water. Within the range $w$ = 12–20, the backbone motions continue to increase in amplitude

and possibly frequency with the result that $T_1$ for $^{31}P$ passes through a shallow minimum at $w = \sim 20$. The narrowing of the $^{31}P$ spectrum, which began with uptake of the first moles of water and then leveled off, becomes more distinct at this level of hydration. As shown in Figure 3, the deuterium spectra shows pronounced broadening of the horns, but the spectrum remains nearly full width as intensity is lost.

Above $w = 20$, free water starts to fill the grooves of DNA, and water added between the DNA helices makes the sample swell (Falk et al., 1962). The $^{31}P$ spectrum was found (Mai et al., 1983) to narrow rapidly to a line of essentially Lorentzian shape, and simultaneously the $^{31}P$ $T_1$ was found to increase gently. The deuterium $T_1$ also appears to decrease more gently above $w = 20$, but the rapid loss of signal prevents the detection of a possible $T_1$ minimum. Both bases and backbone clearly undergo large-angle motion in this range of hydration, and as suggested previously (Bendel et al., 1983; James et al., 1983; Mai et al., 1983), this additional motion must be dominated by low-frequency fluctuations since the spectrum disappears, while $T_1$ is relatively unaffected (Woessner et al., 1969). It is interesting to note, however, that the $^2H$ spectrum *is* observable at higher water levels in oriented liquid-crystalline samples of short DNA fragments (Brandes & Kearns, 1986).

Up to $w = 20$, the ratio of $^{31}P$ and $^2H$ $T_1$ values is approximately constant, implying that the base motion is coupled to that of the backbone. This parallel in the behavior of the $^2H$ and $^{31}P$ $T_1$ values appears to be independent of the A/B conformational state since the Na-DNA samples of Mai et al. (1983) probably converts from the A to B form at $w = 12$–13, whereas our Li-DNA remains in the B-form throughout the hydration range. Moreover, our limited measurements on Na-DNA (see Table I) are, within experimental error, about the same as Li-DNA even though the Na-DNA is in the A form below $w = 10$ and in the B form at $w = 21$.

Provided that the molecular motion is fast on a time scale defined by the rigid lattice quadrupolar splitting, the deuteron spin–lattice relaxation time is given by the relation

$$T_1^{-1} = R_1 = \frac{3\pi^2}{2}(\langle e^2qQ/h\rangle_0)^2[J_1(\omega_0) + 4J_2(2\omega_0)] \quad (7)$$

where $R_1$ is the spin–lattice relaxation rate of the Zeeman polarization for a deuteron in a given orientation. In eq 7 it is assumed that $\eta = 0$ and that the quadrupole coupling constant $\langle e^2qQ/h\rangle_0$ has been averaged over those vibrational motions that are too fast to produce relaxation. $J_1$ and $J_2$ are two different spectral density functions that are evaluated at the indicated multiples of the Larmor frequency $\omega_0$. In order to apply eq 7 to solid samples, it must be recognized that $J_1$ and $J_2$ depend on the orientation of the CD bond with respect to the magnetic field. Thus, the $J_M(M\omega_0)$ of eq 7 may be written (Freed, 1977):

$$J_M(M\omega_0,\beta) = \sum_{N=-2}^{2} [d^{(2)}_{MN}(\beta)]^2 J_N(M\omega_0,0) \quad (8)$$

where $\beta$ now refers to the angle between the CD bond and the magnetic field and the geometric factors $d^{(2)}_{MN}(\beta)$ are the reduced second-rank Wigner rotation matrix elements (Brink & Satchler, 1975). The $J_N(M\omega_0,0)$ now refer to spectral densities measured at $\beta = 0$. In the present case, where we have measured $T_1$ for the horns of the powder patterns, the observed recovery curves are a weighted average consisting of 63.4% from spins at $\beta = 90°$ and 36.4% from spins with $\beta = 35.5°$.

We attempted to analyze the deuteron relaxation data in Figure 5 in terms of the diffusion-in-a-cone model (Warchol & Vaughan, 1978; Wang & Pecora, 1980). This is the simplest model of anisotropic motion that might be expected to account for the DNA relaxation behavior. Provided that the cone angle $\theta_0$ is less than 60° (Wang & Pecora, 1980), the spectral densities on the right-hand side of eq 8 are given by single Lorentzian expressions of the form

$$J_N(M\omega_0,0) = C_N \frac{b_N/D_R}{1 + (M\omega_0)^2(b_N/D_R)^2} \quad (9)$$

$D_R$ is the rotational diffusion constant from which we may define a correlation time $\tau_N \equiv b_N/D_R$, and the coefficients $C_N$ are the amplitudes of the appropriate correlation functions. In the limit of unrestricted diffusion over a sphere, the $C_N$ and $b_N$ reduce to 1/5 and 1/6, respectively. Lipari and Szabo (1981) have derived approximate, but highly accurate, analytical expressions for the coefficients $C_N$ and $b_N$, as a function of the cone angle $\theta_0$.

Equations 8 and 9 show that three distinct correlation times are required to describe the relaxation behavior, even for cones with $\theta_0 < 60°$. Given the relatively large number of Lorentzians that enter into the expression for $R_1$ through eq 7–9, it seemed possible that we might be able to fit the experimentally observed frequency dependence of the relaxation times. We consequently evaluated the coefficients appearing in eq 7–9 as well as $T_1$ as a function of $\theta_0$, $D_R$,$\beta$ and $\omega_0$. The observed quadrupolar splittings limit the range of possible cone angles to 0–16°, and the observation of frequency-dependent $T_1$'s eliminates solutions with $(M\omega_0\tau_N)^2 \ll 1$ from consideration. Within these limits, it is impossible to find any values of the cone correlation times that satisfy the constraint that $T_1(76.8)/T_1(38.4) = 2.0 \pm 0.4$, which is imposed by the data in Table I.

Further attempts to simulate the observed deuterium relaxation behavior with other restricted diffusion models fail for essentially the same reason: it is not possible with any model that leads to a limited number of exponential correlation functions to explain how $T_1$ can change by a factor of 10 on going from drier to wetter samples while maintaining a roughly constant factor of 2 for the ratio $T_1(76.8)/T_1(38.4)$.

An attractive alternative to the restricted diffusion models incorporates collective torsional modes as a major component of the internal motion in duplex DNA (Allison et al., 1982). According to this type of model, the motion of individual C–D vectors reflects coupled torsional modes involving many base pairs. Using this model, Allison and Schurr (1979) have obtained explicit expressions for correlation functions that explain fluorescence depolarization data of DNA solutions, and they have also shown (Allison et al., 1982) that collective torsional deformations can account reasonably well for $^{31}P$ relaxation data.

Models involving collective fluctuations always lead to a (well-defined) distribution of correlation times, and the particular distribution that appears in the Allison–Schurr theory yields expressions for the frequency dependence of the relevant spectral densities, which are, in general, quite complicated. However, for a wide range of values of the effective elastic constant and frictional coefficient that appear in the Allison–Schurr formulas, the frequency dependence reduces to the simple form $\omega_0^{-1/2}$. This is similar to models of collective fluctuations developed previously (Pincus, 1969; Doane et al., 1974) to account for spin relaxation in thermotropic liquid crystals. Here it was recognized (Blinc, 1976) that particular relations between the elastic constants associated with different types of deformations may cause the frequency dependence to change from $\omega_0^{-1/2}$ to $\omega_0^{-1}$. The result is an effective change

in dimensionality of the elastic deformations that has been suggested as a proper description (Marquese et al., 1984) of the coherent fluctuations responsible for relaxation of spins in lipid bilayers (Brown, 1984).

If collective torsional fluctuations are the dominant source of spin–lattice relaxation in hydrated DNA fibers, the rapid decrease of both $^{31}P$ and $^{2}H$ relaxation times could be ascribed to water molecules acting to decrease the effective elastic constant for torsional deformations. Moreover, the very low frequency end of the motional spectrum will involve a distribution of torsional modes, which may well account for both the $^{2}H$ and the $^{31}P$ line shapes [at least prior to the onset of full reorientation, which seems to occur (Fujiwara & Shindo, 1985; H. Shindo, Y. Hiyama, S. Roy, J. S. Cohen, and D. A. Torchia, unpublished results) in samples hydrated at 98% RH]. In order to definitively test for the presence of collective modes as a source of deuteron relaxation in DNA fibers, it would be desirable to measure the relaxation rates over a much wider range of frequencies. Alternatively, equally definitive tests can be made on the basis of the determination of individual spectral densities (Jacobsen & Schaumburg, 1976; Vold & Vold, 1977) in oriented DNA fibers. Such measurements are in progress in our laboratory.

## SUMMARY

The measurements reported in this paper have shown that a strong correlation exists between relaxation rates for deuterium in the base pairs and previously reported backbone $^{31}P$ relaxation data. Although our data are limited, the observation of a relatively constant ratio of 2 between relaxation times measured at 76.8 and 38.4 MHz eliminates simple exponential correlation functions from consideration as the dominant contribution to the deuterium relaxation rates. As discussed earlier (Allison & Schurr, 1979; Allison et al., 1982), the internal motion is more likely to be coherent in nature, with the DNA fibers behaving essentially as elastic filaments. The predictions of such models for the motion may be tested by more detailed relaxation measurements, in particular by determination of individual spectral densities of motion.

## ACKNOWLEDGMENTS

We thank Dr. James Yesinowski for his kind help in recording the 76.8-MHz deuterium spectra. We are particularly grateful to Drs. Y. Hiyama and H. Shindo for sending us a preprint of their unpublished results.

## REFERENCES

Allison, S. A., & Schurr, J. M. (1979) *Chem. Phys. 41*, 35–59.
Allison, S. A., Shibata, J. H., Wilcoxon, J., & Schurr, J. M. (1982) *Biopolymers 21*, 729–762.
Assa-Munt, N., Granot, J., Behling, R. W., & Kearns, D. R. (1984) *Biochemistry 23*, 944–955.
Barkley, M. D., & Zimm, B. H. (1979) *J. Chem. Phys. 70*, 2991–3007.
Barnes, R. G. (1976) *Adv. Pure Quad. Res. 1*, 335.
Bendel, P., Murphy-Boesch, J., & James, T. L. (1983) *Biochim. Biophys. Acta 759*, 205–213.
Blinc, R. (1976) *NMR: Basic Princ. Prog. 13*, 97.
Bloom, M., Davis, J. H., & Valic, M. I. (1980) *Can. J. Phys. 58*, 1510.
Bolton, P. H., & James, T. L. (1980) *J. Am. Chem. Soc. 102*, 25–31.
Brandes, R., & Ehrenberg, A. (1986) *Nucleic Acids Res.* (submitted for publication).
Brandes, R., & Kearns, D. R. (1986) *Biochemistry* (in press).
Brink, D. M., & Satchler, G. R. (1975) in *Angular Momentum*, Oxford University Press (Clarendon), London.
Brown, M. F. (1984) *J. Chem. Phys. 80*, 2808.
Cohen, A., & Eisenberg, H. (1969) *Biopolymers 8*, 45.
Davis, J. H., Jeffrey, K. R., Bloom, M., & Valic, M. I. (1976) *Chem. Phys. Lett. 42*, 390–394.
DiVerdi, J. A., & Opella, S. J. (1981) *J. Mol. Biol. 149*, 307–311.
Doane, J. W., Tarr, C. E., & Nickerson, M. A. (1974) *Phys. Rev. Lett. 33*, 620.
Drew, H., Takano, T., Tanaka, S., Itakura, K., & Dickerson, R. E. (1980) *Nature (London) 286*, 567–573.
Drew, H. R., Samson, S., & Dickerson, R. E. (1982) *Proc. Natl. Acad. Sci. U.S.A. 79*, 4040–4044.
Early, T. A., Kearns, D. R., Hillen, W., & Wells, R. D. (1981) *Biochemistry 20*, 3756–3764.
Englander, S. W., Kallenbach, N. R., Heeger, A. J., Krumhansl, J. A., & Litwin, S. (1980) *Proc. Natl. Acad. Sci. U.S.A. 77*, 7222–7226.
Falk, M., Hartman, K. A., & Lord, R. C. (1962) *J. Am. Chem. Soc. 84*, 3843–3846.
Falk, M., Hartman, K. A., & Lord, R. C. (1963) *J. Am. Chem. Soc. 85*, 387–391.
Freed, J. H. (1977) *J. Chem. Phys. 66*, 4183–4199.
Fujiwara, T., & Shindo, H. (1985) *Biochemistry 24*, 896–902.
Hogan, M. E., & Jardetzky, O. (1980) *Biochemistry 19*, 3460–3468.
Holbrook, S. R., & Kim, S.-H. (1984) *J. Mol. Biol. 173*, 361–388.
Jacobsen, J. P., & Schaumburg, K. (1976) *J. Magn. Reson. 24*, 173.
James, T. L., Bendel, P., James, J. L., Keepers, J. W., Kollman, P. A., Lapidot, A., Murphy-Boesch, J., & Taylor, J. E. (1983) in *Nucleic Acids: The Vectors of Life* (Pullman, B., & Jortner, J., Eds.) pp 155–167, Reidel, Dordrecht, Holland.
Kearns, D. R. (1984) *CRC Crit. Rev. Biochem. 15*, 237–290.
Keepers, J. W., & James, T. L. (1982) *J. Am. Chem. Soc. 104*, 929–939.
Levy, G. C., Craik, D. J., Kumar, A., & London, R. E. (1983) *Biopolymers 22*, 2703–2726.
Lindsey, S. M. (1986) in *Computer Analysis for Life Science*, Ohm, Tokyo (in press).
Lipari, G., & Szabo, A. (1981) *J. Chem. Phys. 75*, 2971–2976.
Mai, M. T., Wemmer, D. E., & Jardetzky, O. (1983) *J. Am. Chem. Soc. 105*, 7149–7152.
Marquese, J. A., Warner, M., & Dill, K. A. (1984) *J. Chem. Phys. 81*, 6404.
Nall, B. T., Rotwell, W. P., Waugh, J. S., & Rupprecht, A. (1981) *Biochemistry 20*, 1881–1887.
Opella, S. J., Wise, W. B., & DiVerdi, J. A. (1981) *Biochemistry 20*, 284–290.
Pincus, P. (1969) *Solid State Commun. 7*, 415.
Rupprecht, A., & Forslind, B. (1970) *Biochim. Biophys. Acta 204*, 304–316.
Shindo, H., Wooten, J. B., Pheiffer, B. H., & Zimmerman, S. B. (1980) *Biochemistry 19*, 518–526.
Shindo, H., Matsumoto, H., Akut, H., & Fujiwara, T. (1983) in *Nucleic Acids: The Vectors of Life* (Pullman, B., & Jortner, J., Eds.) pp 169–182, Reidel, Dordrecht, Holland.
Shindo, H., Fujiwara, T., Akutsu, H., Matsumoto, U., & Kyogoku, Y. (1985) *Biochemistry 24*, 887–895.
Thomas, J. C., & Schurr, J. M. (1983) *Biochemistry 22*, 6194–6198.
Tsang, P., Vold, R. R., & Vold, R. L. (1986) *J. Magn. Reson.* (in press).
Vold, R. R., & Vold, R. L. (1977) *J. Chem. Phys. 66*, 4018.

Vold, R. R., Brandes, R., Tsang, P., Kearns, D. R., Vold, R. L., & Rupprecht, A. (1986) *J. Am. Chem. Soc. 108*, 302–303.
Wang, C. C., & Pecora, R. (1980) *J. Chem. Phys. 72*, 5333–5340.
Warchol, M. P., & Vaughan, W. E. (1978) *Adv. Mol. Relax. Interact. Processes 13*, 317–330.
Weast, R. C. (1971) in *Handbook of Chemistry and Physics*, 52nd ed., p D-214, The Chemical Rubber Co., Cleveland, OH.
Woessner, D. E., Snowden, B. S., & Meyer, G. H. (1969) *J. Chem. Phys. 51*, 2968–2976.

# $^{15}N$ NMR Spectroscopy of Hydrogen-Bonding Interactions in the Active Site of Serine Proteases: Evidence for a Moving Histidine Mechanism†

William W. Bachovchin
*Department of Biochemistry and Pharmacology, Tufts University School of Medicine, Boston, Massachusetts 02111*
*Received May 21, 1986; Revised Manuscript Received August 18, 1986*

ABSTRACT: Nitrogen-15 NMR spectroscopy has been used to study the hydrogen-bonding interactions involving the histidyl residue in the catalytic triad of α-lytic protease in the resting enzyme and in the transition-state or tetrahedral intermediate analogue complexes formed with phenylmethanesulfonyl fluoride and diisopropyl fluorophosphate. The $^{15}N$ shifts indicate that a strong hydrogen bond links the active site histidine and serine residues in the resting enzyme in solution. This result is at odds with interpretations of the X-ray diffraction data of α-lytic protease and of other serine proteases, which indicate that the serine and histidine residues are too far apart and not properly aligned for the formation of a hydrogen bond. In addition, the nitrogen-15 shifts demonstrate that protonation of the histidine imidazole ring at low pH in the transition-state or tetrahedral intermediate analogue complexes formed with phenylmethanesulfonyl fluoride and diisopropyl fluorophosphate triggers the disruption of the aspartate–histidine hydrogen bond. These results suggest a catalytic mechanism involving directed movement of the imidazole ring of the active site histidyl residue.

The active sites of serine proteases invariably contain a particular arrangement of the side-chain functional groups of aspartic acid, histidine, and serine known as the "catalytic triad" or "charge-relay" system (**1a**). How this triad functions

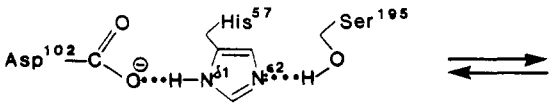


*1a*

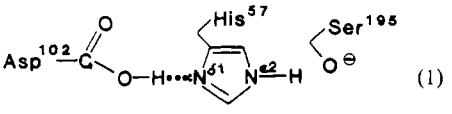


(1)

*1b*

in catalysis is an old problem, which despite extensive effort has not been solved.

Central to the problem is the question of whether or not a H-bond[1] links $N^{\epsilon 2}$ of His-57 and $O^{\gamma}$ of Ser-195 in the resting enzyme at catalytically active pH (>7.0). X-ray diffraction studies of chymotrypsin (Blow et al., 1969) and of other serine proteases (Kraut, 1977) were first interpreted as indicating that this H-bond is formed, along with a second H-bond between His-57 and Asp-102 as shown in **1a**. This finding of a H-bonded network linking Asp-102, His-57, and Ser-195 prompted Blow to postulate his charge-relay theory in which he argued that the unusual reactivity of the active site serine—the hallmark of serine proteases—could be understood in terms of the generation of a serine alkoxide ion (**1b**). Negative charge, according to this scheme, is in effect transferred from the carboxylate anion of Asp-102 to the serine via the H-bonding network (eq 1).

Blow's charge-relay theory, as originally formulated and understood by others in the field, had a number of deficiencies and did not gain much support. However, a modified charge-relay scheme proposed by Hunkapiller and co-workers (Hunkapiller et al., 1973) did gain wider acceptance. In this scheme, attack of the serine hydroxyl group on the carboxyl carbon of the substrate is accompanied by the concerted transfer of two protons: the serine hydroxyl proton to $N^{\epsilon 2}$ of His-57 and the $N^{\delta 1}$ proton of His-57 to the carboxylate anion of Asp-102, as shown in eq 2. The experimental basis for this proposal came from a measurement of the spin coupling between the histidyl's $C^{\epsilon 1}$ carbon and its attached proton, which indicated that the imidazole ring had an abnormally low $pK_a$—lower in fact than that of the carboxylate of Asp-102,

† Supported by Research Grant GM 27927 and Research Career Development Award AM 01122 from the National Institutes of Health, by Equipment Grant PCM-8212656 from the National Science Foundation, and by NIH Research Resource Grant RR-02231. Presented in part at the 11th International Conference on Magnetic Resonance in Biological Systems, Goa, India, Sept 17–23, 1984, at the 188th National Meeting of the American Chemical Society, Philadelphia, PA, Aug 26–31, 1984, and at the 4th Conversation in the Discipline—Biomolecular Stereodynamics, State University of New York at Albany, June 4–8, 1985.

[1] Abbreviations: H-bond, hydrogen bond; PMSF, phenylmethanesulfonyl fluoride; DIFP, diisopropyl fluorophosphate; TI, tetrahedral intermediate; SPGA, *Streptomyces griseus* protease A; Tris, tris(hydroxymethyl)aminomethane.

0006-2960/86/0425-7751$01.50/0 